# In silico analysis of potential Tankyrase I inhibitors for ovarian cancer

By

Naishik Ovrha Farouqe

22146054

A thesis submitted to the School of Pharmacy in partial fulfillment of the requirements for the degree of Bachelor of Pharmacy (B. Pharm.)

School of Pharmacy
BRAC University
May,2026

## Declaration

It is hereby declared that

1. The thesis submitted is my/our own original work while completing degree at Brac University.
2. The thesis does not contain material previously published or written by a third party, except where this is appropriately cited through full and accurate referencing.
3. The thesis does not contain material which has been accepted, or submitted, for any other degree or diploma at a university or other institution.
4. I have acknowledged all main sources of help.

**Naishik Ovrha Farouqe**
22146054

## Approval

The thesis entitled **"In silico analysis of potential Tankyrase I inhibitors for ovarian cancer"** submitted by Naishik Ovrha Farouqe, of Summer 2022 has been accepted as satisfactory in partial fulfillment of the requirement for the degree of Bachelor of Pharmacy.

**Examining Committee:**

**Supervised By**:

Luluel Maknun Fariha
Senior Lecturer
BRAC University

Namara Mariam Chowdhury
Senior Lecturer
BRAC University

Nashrah Mustafa
Senior Lecturer
BRAC University

**Approved By:**

Dr. Sharmind Neelotpol
Professor & Chairperson
BRAC University

## Ethics Statement

This project does not involve any kind of animal and human trial.

## Dedication

This work is for all cancer patients who bravely battle their disease with strength, hope & courage. This is especially for those of you that fight ovarian cancer, the silent sounds of your battle and strength propels research and discoveries. May this work, in some small way, help us move towards more evidence-based knowledge of our condition and treatments, and shines forth hope for better outcomes and hope for brighter futures.

## Acknowledgement

I would like to thank Allah (SWT) the Most Gracious and the Most Merciful for giving me strength, patience, and knowledge to finish this work. I could have never achieved this without His guidance and blessings. I am genuinely grateful for the endurance and courage, He has given me during this entire journey.

I would also like to extend my sincere thanks to Ms. Luluel Maknun Fariha and Namara Mariam Chowdhury for her invaluable support and guidance throughout the completion of this thesis, her guidance during this thesis was not only insightful but transformative, shaping my understanding and refining my approach to research. Beyond this, her presence over the past four years of undergraduate study through every course, has been deeply impactful. Her dedication to teaching and her belief in her students have left a lasting impression on me, for which I remain sincerely grateful.

# In silico analysis of potential Tankyrase I inhibitors for ovarian cancer


## Abstract

In this study, we aimed to identify repurposed small-molecule inhibitors of Tankyrase-1 by combining molecular docking with pharmacokinetic and drug-likeness profiling. We screened four thousand assorted subjects including the semi-synthetic isoquinoline alkaloid Hydrastinine, the orally active P-selectin antagonist PSI-697, the irreversible monoamine oxidase inhibitor Benmoxin and the investigational anxiolytic α7-nicotinic receptor modulator BNC-210. For docking, we predicted that Benmoxin is multi-point anchored within the Tankyrase-1 catalytic pocket by its interactions with residues Pro1235 (double-headed arrow in (Figures 3B and 3D), Pro1187 and Tyr1226, whilst PSI-697 appeared to only interact with Pro1235 and Tyr1226. Hydrastinine and BNC-210, by contrast, were predicted to bind Pro1235 and Pro1187 whilst showing a loss of the Tyr1226 interaction. Benmoxin (multi-residue binding) and PSI-697 (contacting Tyr1226) showed the best relative docking stabilities.

All four of the ligands were predicted to pass Lipinski's rule of five and have high gastrointestinal absorption according to SwissADME. For Benmoxin and BNC-210 LogP values were moderate (≈2.6), high for PSI-697 (≈4.3) and low for Hydrastinine (≈1.2). PSI-697, Benmoxin and BNC-210 were predicted to cross the blood–brain barrier (BBB), while Hydrastinine was not. Hydrastinine and BNC-210 were predicted as P-glycoprotein efflux substrates (risk of efflux), whereas PSI-697 or Benmoxin were not. Hydrastinine was found to have low predicted cytochrome P450 inhibition, Benmoxin to inhibit only CYP2D6 and PSI-697 and BNC-210 predicted broad (multiple isoforms) inhibition. Hydrastinine remained within the intestinal-absorption compartment in the BOILED-Egg model, while PSI-697, Benmoxin and BNC-210 permeated across the blood brain barrier.

## Table of Contents

**List of Tables**

## List of Figures



## Introduction

### 1.1 Prevalence

Ovarian cancer globally ranks as the eighth leading form of cancer and cancer mortality affecting roughly 324,398 in 2022 and claiming around 206,328 lives worldwide.(Caruso et al., 2025) In Bangladesh, 3122 new cases and 2096 deaths have been reported by GLOBACAN in the year 2020 having an incidence rate of 3.9% and mortality rate 2.9%, ranking 15th amongst other forms of cancer.(Filho et al., 2025) A large variation is seen regarding the incidence of ovarian cancer in different parts of the world with the highest prevalence observed amongst non-Hispanic white women (12.0 per 100,000), followed by Hispanic (10.3 per 100,000), non-Hispanic black (9.4 per 100,000), and Asian/ Pacific Islander women (9.2 per 100,000).(La Vecchia, 2001; Momenimovahed et al., 2019) Due to limitation in cancer diagnostics and therapeutic services mortality rate is the highest in African populations.(Chornokur et al., 2013)

### 1.2 Background

Ovarian cancer is one of those diseases having a highly lethal gynecological malignancy which is marked by delayed diagnosis, recurrence, and therapeutic resistance. Molecular mechanisms which are involved in ovarian cancer are the Wnt/β-catenin signaling pathway implicated in the initiation, proliferation and development of the tumor as well as the metastasis. Regulating this

pathway is the Tankyrase I (TNKS1) enzyme which is a member of the PARP family. It shows its mechanism of action by promoting the degradation of Axin i.e a crucial part of the β-catenin destruction complex which furthermore leads to stabilization and activation of β-catenin signaling. Studies have revealed activation of Tankyrase in ovarian cancer, thereby enhancing tumor progression and metastasis through this Wnt/β-catenin signaling.

### 1.3 Types and Classification of ovarian cancer

Ovarian cancer can be divided into two types, Type I and Type II where Type I are generally slow growing and idle meanwhile Type II ones are aggressive neoplasm.(Koshiyama et al., 2017) TypeI ovarian cancers include Endometrioid Carcinoma, Clear Cell Carcinoma, Mucinous Carcinoma, and rarely occurring Low-Grade Serous Carcinoma. All these subtypes of cancer are all different when it comes to their etiology, morphology, molecular biology and prognosis, but they are treated as a single cluster.(Kossaï et al., 2018) This class of cancer show somatic mutations in the KRAS, BRAF or ERBB2 genes but they somehow lack TP53 mutations in the TP53 genes. In the early stage they arise from neoplastic lesions in a stepwise manner and are somewhat slow in progression but they can be diagnosed at an early stage.(Vang et al., 2009) In addition Type II High-Grade Serous Carcinoma is an example of Type II ovarian cancer and it has the worst prognosis as they are detected well into the advanced stage.(Cho & Shih, 2009; Koshiyama et al., 2017) These tumors show frequent/recurrent mutations in specific oncogenes including a pathognomonic mutation of TP53.(Vang et al., 2009)

For the treatment of the patients suffering from various subtypes of cancer a classification system is a must for appropriate clinical management and recovery. However, this 2-tier system is quite oversimplified, as tumors with different morphological and genetic characteristics are grouped together in the same class. Even from a clinical standpoint, type I tumors which are diagnosed at a late stage similarly have a slow prognosis like type II tumors.(Braicu et al., 2011)

Primary characteristics of the 5 histotypes of ovarian cancer are discussed in the following paragraphs.

**Serous Carcinomas**

High-Grade Serous Carcinoma

Amongst Epithelial carcinomas, Serous carcinomas (SC) make up around 75–80% and it is further divided into two types, High Grade Serous Carcinoma (HGSC) and Low-Grade Serous Carcinoma (LGSC). 85–90% of SC is composed of HGSC, in addition prevalence is mostly observed in elderly patients. However, they are responsible for causing the most fatalities as they are detected well into the advanced stage. From a morphological perspective, HGSC consists of cells which are ciliated and columnar cells forming solid masses, or slit-like spaces with high-grade nuclear atypia and >12 mitoses/10 HPF. Various genomic mutations, including BRCA1/ BRCA2 and TP53 have been linked to HGSC statistically around 22% meanwhile 6 other recurrently mutated genes have been observed but with a relatively low percentage around less than 10%.(Malpica et al., 2004)

Low-Grade Serous Carcinoma

Compared to HGSC, LGSC are relatively rare, consisting of around 10–15% of SC and 2% amongst ovarian carcinomas. Unlike HGSC, they can be diagnosed at a younger age. Even though they lack atypia, morphologically they are quite similar to HGSC having a greater than <12 mitoses/10 HPF. Molecular analyses have shown, LGSC have been linked to somatic mutations in KRAS and BRAF genes observed in almost half of the cases(Malpica et al., 2004; Mayr et al., 2006).

**Mucinous Carcinomas**

Mucinous Carcinomas (MC) previously known as intestinal-type carcinomas, are a rare type of carcinoma having a prevalence rate of around to 2–3% of ovarian carcinomas. Diagnosis is possible at an early stage for these types of patients and the prognosis rate after surgery is quite

good.(Ludwick et al., 2005; Rodríguez & Prat, 2002).These types of carcinomas have big, unilateral, multicystic tumors, which are solid in some places and are often packed with mucus. In a morphological perspective, mucinous carcinomas have varying sizes of cysts and glands having a confluent shape with successive glands. Tall, columnar, and stratified, these cells are equipped with a large cytoplasm containing a protein named mucin.(Ludwick et al., 2005) Mucinous carcinomas are prevalent with KRAS mutations, with a rate of 75% in primary MC. These are observed in benign and in borderline areas and their tumorigenesis process starts from a low-grade malignant mucinous lesion to an MC.

**Endometrioid Carcinoma**

Of all ovarian carcinomas, this type of carcinomas account for around 10% and are usually unilateral solid masses. They have a good prognosis as well as present at a low grade. Endometrioid carcinoma shows positivity for CK7, PAX8, and hormone receptors, and negative results for WT1 and CK20 in the immunohistochemistry profile. Additionally, in high grade EC p53 can be overexpressed. EC has the highest prevalence amongst patients with Lynch syndrome. Furthermore, in rare cases microsatellite instability has been observed.(Lu et al., 2012)

**Clear-Cell Carcinomas**

Out of all EOC, Clear Cell Carcinoma have a prevalence rate around 3.7 to 12.1% and they have the worst prognosis shown by earlier studies.(Lee et al., 2011) These tumors often manifest as a large pelvic mass and sometimes occur bilaterally.(Kobayashi et al., 2009) Unlike SC, WT1, p53, and ER genes are not expressed by CCC they particularly express napsin A, in contrast to the other EOC.(Yamashita et al., 2015) Other studies have documented that in half of all cases, the tumor suppressor ARID1A is mutated. Likewise, mutations in PI3KCA have also been reported.(Jones et al., 2010; Kuo et al., 2009)

On a positive note, throughout the last two decades advances in chemotherapy , targeted therapy, and immunotherapy which includes platinum based therapy, using monoclonal antibodies such as Bevacizumab and more recent treatments such as Mirvetuximab Soravtansinean and Fam-Trastuzumab Deruxtecan-nxki has led to decreased mortality in patients with advanced ovarian cancer.(Kuo et al., 2009; Moore et al., 2023).Ovarian cancer treatments have come a long way from Cisplatin, the first platinum based chemotherapy agent to aforementioned therapies. Cisplatin used in the mid1970s but due to their toxic side effects such as nephrotoxicity, neurotoxicity lead to the development of 2nd generation Carboplatin.[26]

**1.4 Mechanism of Action**

One of the most significant mechanisms involved in ovarian cancer is Wnt/*β*-catenin pathway which play a crucial role in proliferation, differentiation and metastasis.(Mitra & Roy, 2017) When Wnt ligands bind to cell-surface receptors it results in the activation of the Wnt signalling pathway due to the stabilization of β-catenin.(Kikuchi, 2003). There are plenty of proteins involved downstream in the pathway including Snail (*SNAIL*), Axin2 (*AXIN2*), and matrix metalloproteinases (*MMPs*)(R. C. Arend et al., 2013).

The canonical Wnt/β-catenin pathway, the non-canonical planar cell polarity pathway, and the non-canonical Wnt–Ca2+ pathway are the three primary Wnt signaling pathways. These pathways can be classified into two categories: canonical or non-canonical. The presence or lack of β-catenin is the differentiating factor between them.(Rebecca C. Arend et al., 2013)

Wnt proteins consist of a class of 19 cysteine-rich glycoproteins, which function as ligands for the Wnt signaling pathway [24]. Three signaling pathways are activated after the proteins bind to the Frizzled (Fzd) transmembrane receptor; these include the canonical Wnt/β-catenin pathway and two canonical pathways. Furthermore, this binding leads to the recruitment of Dishevelled (Dsh) protein in all the pathways mentioned. In the Wnt/$Ca^{2+}$ non-canonical pathway, the complex which was Wnt/Fzd/Dsh combines with another protein named G protein (Ror1/2),

which triggers the activation of calmodulin-dependent kinase II (CaMKII), protein kinase C (PKC), and calcineurin, which causes the intracellular calcium levels to increase and downstream signaling. This signaling pathway is crucial for embryonic development of various organs, one of them being the ovaries (Harris et al., 2012).

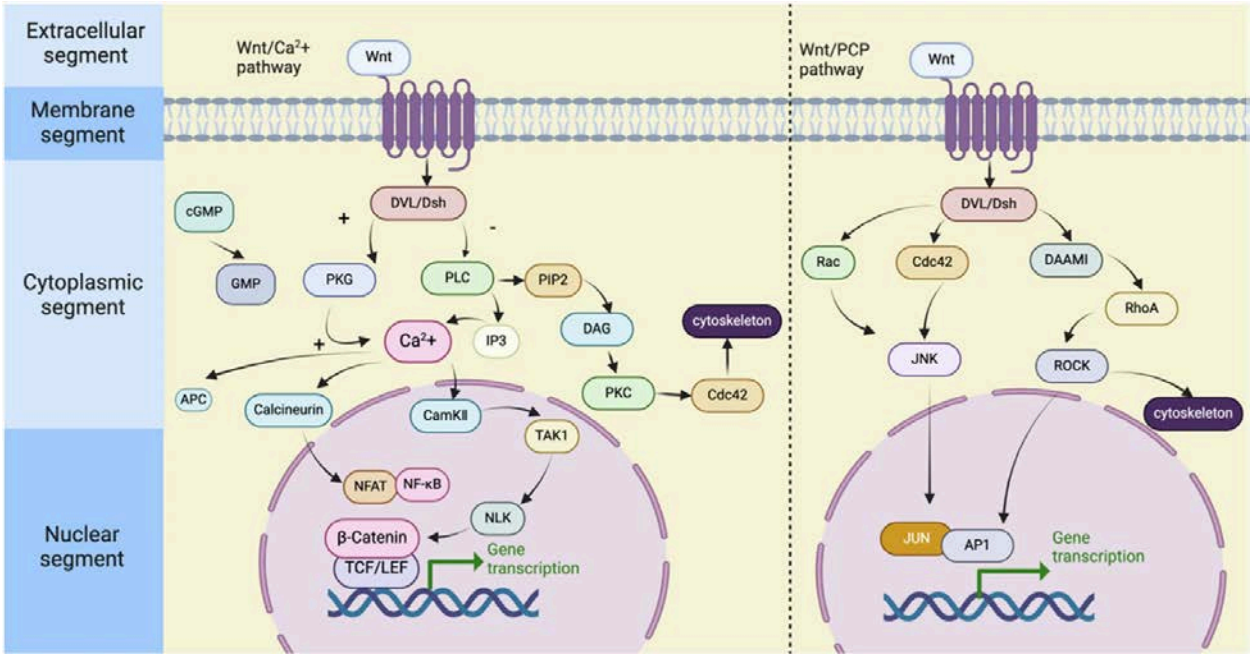


***Fig1****: The mechanism of canonical Wnt pathway.*

Depending on the Wnt ligand's availability and receptor engagement, the canonical Wnt/β-catenin pathway has two operating modes, "off" (inactive) and "on" (active). In the "off" stage of the pathway, due to the absence of Wnt, lack of receptor availability, or inhibition by antagonists Wnt ligands do not bind to their receptors. This is further prevented, after the Dikkopf family (DKK1–4) binds to the transmembrane receptors Frizzled (Fzd) and LRP5/6. Additionally, when Wnt-inhibitory factor-1 (WIF-1) and Frizzled-related proteins (SFRP1–5) bind with Wnt ligands, it also blocks the receptor interactions. β-catenin is disrupted by the destruction complex, consisting of Axin, adenomatous polyposis coli (APC), and glycogen synthase kinase 3β (GSK3β) in the absence of Wnt signaling. It is first phosphorylated by casein kinase 1 (CK1) and GSK3β, furthermore it is then ubiquitinated and degraded by the 26S

proteasome. Low levels of cytoplasmic β-catenin, causes the Groucho to bind with TCF/LEF (T-cell factor/lymphoid enhancer factor) transcription factors, as a result leading to transcriptional repression of Wnt target genes.

Meanwhile when the pathway is “on”, Wnt ligands bind to Fzd receptors and co-receptors LRP5/6 (low-density lipoprotein receptor-related proteins) leading to the activation phosphorylation of LRP5/6 by CK1 and GSK3β, and involvement of Dishevelled (Dsh) to the plasma membrane. β-catenin degradation gets inhibited due to the interaction of Axin with phosphorylated LRP5/6, additionally the destruction complex gets disrupted by Dsh. This leads to the accumulation of β-catenin in the cytoplasm thus transferring into the nucleus. Where, it forms a transcriptional activation complex with co-activators such as B-cell lymphoma 9/Legless (BCL9/LGS) and Pygopus (Pygo) after displacing Groucho from TCF/LEF This complex is responsible for activating transcription of Wnt target genes which are involved in the growth development and survival, such as c-MYC (MYC), Cyclin D1 (CCND1), Survivin (BIRC5), Axin2 (AXIN2), and matrix metalloproteinases (MMPs). So far, more than 100 Wnt target genes have been linked with ovarian cancer meanwhile with 23 reported to be overexpressed in ovarian cancer (Kikuchi et al., 2007).

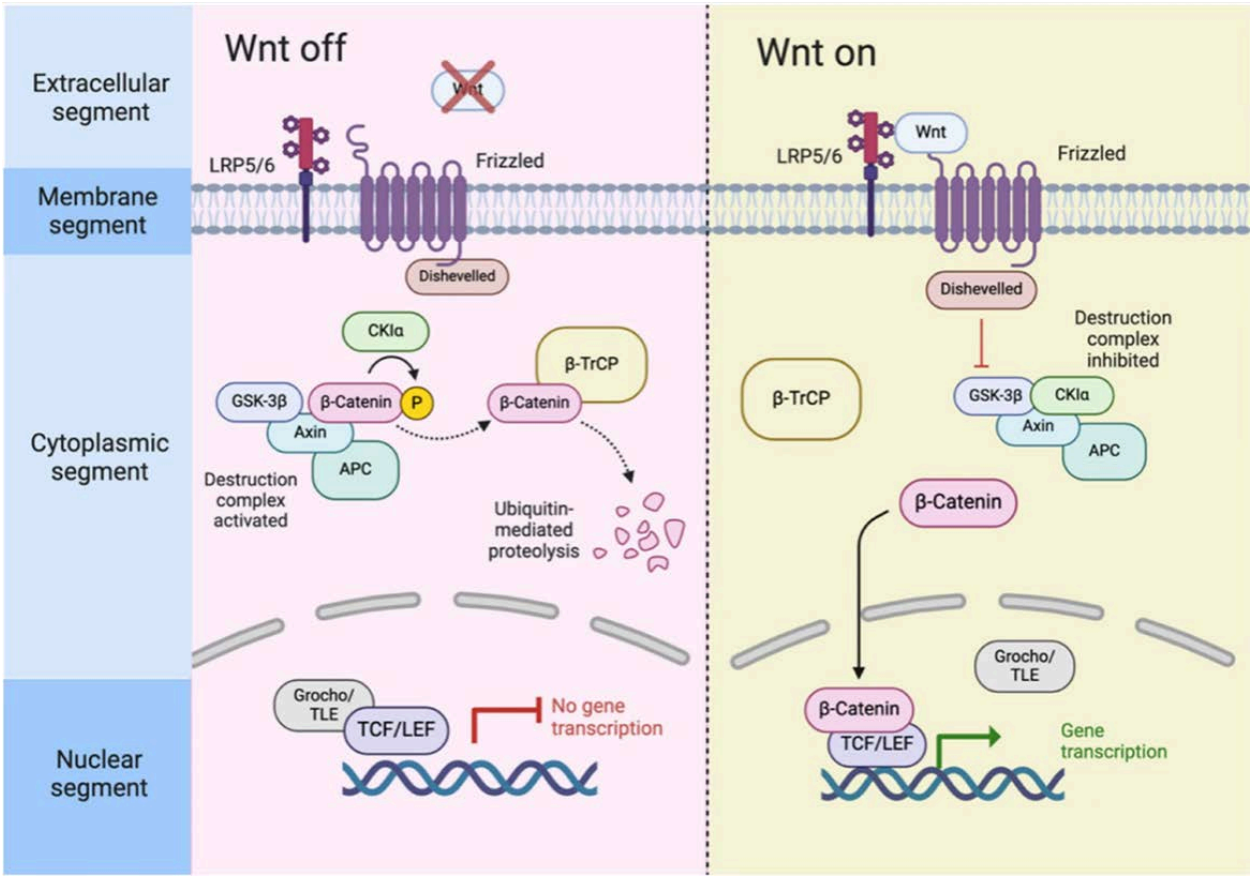


***Fig:2*** *The mechanism of non-canonical Wnt signaling pathways*

### 1.5 Current State of Knowledge

One of the crucial playmakers in the Wnt/*β*-catenin pathway are Tankyrase enzymes, they are part of the diphtheria toxin–like ADP-ribosyltransferase (ARTD) enzyme superfamily where 17 of them are found in humans followed by few in lower eukaryotes, plants, bacteria, and archaea. Tankyrase 1 and Tankyrase 2 also known as PARP5a and PARP5b respectively constitute a unique and separate sub group amongst the polymer-forming ARTDs.(Haikarainen et al., 2014) These two enzymes are key components of the B-catenin destruction complex which plays a key role in promoting the degradation in B-catenin.(Haikarainen et al., 2014) Therefore TNKS can be regarded as a potential and appealing target for anti-ovarian cancer therapy.

Despite TNKS being a relatively new target, a lot of research has been already done, some recent ones include (Haikarainen et al., 2016; Lu et al., 2026; Wang et al., 2025). Several inhibitors of this enzyme has been recognized such as flavone (Narwal et al., 2012), 2-Phenylquinazolinones (Zhu et al., 2024) and a recent novel neoantimycin analog known as UAT-B isolated from *Streptomyces conglobatus* has been able to significantly prevent TNKS–USP25 complex formation, furthermore reduce TNKS levels and prompting cell cycle apoptosis (Zhu et al., 2024)[. In addition, Stenoparib, small-molecule dual-targeted inhibitor of PARP1/2 and Tankyrase 1 and 2 is currently in Phase 2 clinical trial for advanced recurrent ovarian cancer. It is showing prominent benefits, including significant tumor shrinkage and long-term disease stability. (Knudsen et al., 2026).

Nevertheless, the discovery of more highly selective inhibitors is of utmost importance which can be used as a part of combination therapy for ovarian cancers.

### 1.5.1 Importance in the Current Scientific Landscape

Studies have linked dysregulation of the Wnt/β-catenin pathway with various types of cancers, thereby making it a prime therapeutic target. However, due to lack of druggable components effective targeting of this pathway has still remained challenging. Thereby, Tankyrase has risen in ranks as one of the leading targets due its inhibition in stabilizing Axin and downregulating β-catenin signaling. Furthermore, increasing use of computational drug discovery strategies have become quite effective when it comes to identifying and discovering new novel inhibitors thereby reducing time and cost in early-stage drug development.

## 1.6 Scope of the Study

In the following study, using computational techniques we have uncovered potential Tankyrase I inhibitors which are as follows:

- Molecular docking
- Virtual screening
- ADMET prediction

- Molecular dynamic simulations

In recent times, these approaches are being frequently used to forecast binding affinity as well as the pharmacological properties of compounds before experimental validation which are useful in early drug discovery.

### 1.7 Research Gap and Contributions

Even though several Tankyrase inhibitors (e.g., XAV939, IWR-1) have been identified, there are still major hurdles that needs to be overcome, as some of them show toxicity, off-target effects, as well as poor pharmacokinetics (Martins-Neves et al., 2018; Wu et al., 2016). Additionally, ovarian cancer fails to get the limelight as most studies focus on other forms of cancer such as liver, colorectal and breast cancer. Furthermore, a limited integration of computational screening + ovarian cancer-specific targeting exists. For example, studies have revealed Tankyrase's anticancer ability in hepatocellular carcinoma and colorectal cancer models, but ovarian-specific computational screening remains underexplored.

### 1.8 Importance of This Article

**Primary Aim** To identify potential Tankyrase I inhibitors for ovarian cancer using in silico approaches.

**Objectives**

1. Retrieve and prepare TNKS1 protein structure
2. Perform virtual screening of compounds
3. Conduct molecular docking analysis
4. Evaluate ADMET properties
5. Perform molecular dynamics simulations

**Scientific Value**

- Identifies novel drug candidates
- Enhances understanding of structure–activity relationships

- Provides a computational pipeline for drug discovery

**Novelty**

- Focus on ovarian cancer-specific TNKS targeting
- Integration of multiple in silico techniques
- Identification of new potential inhibitors beyond known compounds

**Rationale of the Study**

Chemoresistance and lack of targeted therapies makes it difficult to treat Ovarian cancer. However, due to Tankyrase's role in promoting tumor progression via Wnt signaling has been identified, inhibition of this pathway represents a promising therapeutic strategy. That's why the aim of this study is to find novel inhibitors specific to ovarian cancer

## 2.Methodology

Docking is a computational technique developed by Kuntz et al. (Kuntz et al., 1982) that virtually attempts to predict a complex of two binding partners which are usually biological macromolecules such as proteins or small molecules including endogenous ligands or drugs. At present. specific docking methods are used such as HADDOCK mostly for protein-protein docking (van Zundert et al., 2016). For our research we used a more traditional small-molecule, molecular docking method that is Auto Dock (O. Trott & A. J. Olson, 2010) which is often used to predict ligand interactions with the target protein. In molecular docking, a ligand molecule is placed and aligned inside the binding cavity of the target protein and results are generated for each of the docking poses or conformations displayed as binding affinity having an unit of kcal/mol.

Databases such as RCS Protein Data Bank and Drug Bank were used to get the 3dimensional structures of proteins that were needed for our research. 4000 drugs were used as ligands for this study and they were downloaded from Drug Bank and the macromolecule Tankyrase I (PDB ID: 4W6E) were downloaded from RCS PDB. Software such as Biovia Discovery Studio and PyMol

were used to prepare the receptor following that the ligands as well as the receptor were converted into pdbqt format using Open Babel and other tools including Auto Dock Tools v4 and Auto Dock Vina were employed to determine binding affinities from the ligand-protein interactions and propose best targets against the receptor.(Oleg Trott & Arthur J. Olson, 2010)

The list of softwares used for our research are presented in a tabular structure (Table 1)

| SL | Software & Programs used | Versions | References |
|---|---|---|---|
| 1 | PyMOL | 1.7.4.5 | (Seeliger & de Groot, 2010) |
| 2 | Discovery Studio | 17.2.0.16349 | (Prasada Rao et al., 2023) |
| 3 | Autodock Tools | v4 | (Oleg Trott & Arthur J. Olson, 2010) |
| 4 | Autodock Vina | v1.1 | (Çifci et al., 2012) |
| 5 | Open Babel GUI | 2.4.1 | (O'Boyle et al., 2011) |

*Table 1: Software and programs used in the study*

### 2.1 Macromolecule Preparation

After downloading the 3d confirmation from RCSB Protein Data Bank (https://www.rcsb.org/) in PDB format. The small molecule (3J5) and the water molecules was removed from the structure by PyMol furthermore it was imported in Biovia Drug Discovery Client program from there polar hydrogen and Kollman Charges were added into the molecule. The grid box was set up at 25×25×25 Å and it was centered at their native ligand XYZ coordinates 15.54 × 20.84 × −27.09 for 4W6E. And finally it was converted into .pdbqt format by Open Babel and saved as receptor .pdbqt.

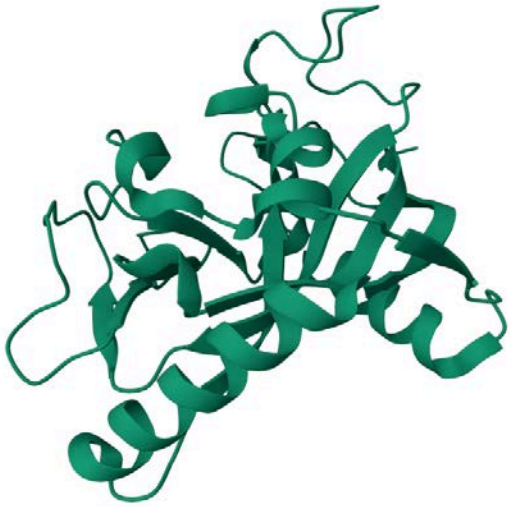

*Fig 3 : 3D Structure of 4W6E*

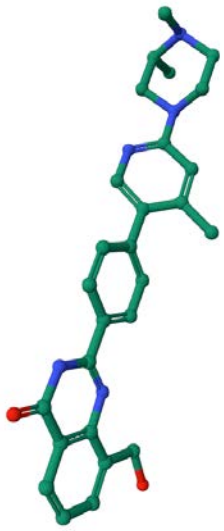

*Fig 4 : 3D Structure of 3J5*

**2.2 Ligand Preparation**

4000 drugs were downloaded from Drug Bank as sd format and all of them were converted into pdbqt format by Open Babel. Furthermore, a split function was used so that each drug compound was saved as an individual pdbqt file. All of them were copied and saved in another folder named Ligand.

**2.3 Auto Dock Vina Analysis**

Since now we have both our macromolecule and ligands ready we can begin molecular docking procedure. Before that we must create a config .txt file where the XYZ coordinates and the gridbox dimensions must be placed. For docking we used Auto Dock Vina which provides algorithms that finds best docking positions between proteins and ligands and then creates output files that contain the binding affinities (usually a negative value) for the best interaction

positions. A maximum of 10 conformers was generated for each ligand and the conformation with the least free binding energy between the ligand and the protein was selected. The following were then selected for analyzing interactions in Biovia Discovery Studio visualizer.

Auto Dock Vina with standard protocol was used to dock the macromolecule Tankyrase I (PDB ID: 4W6E) and 4000 ligands into the active site of proteins. The molecular docking studies were carried out using Auto Dock Tools (ADT) which is a free graphic user interface (GUI) for the AutoDock Vina program. The grid box was constructed using 25x25x25, pointing in x, y, and z directions, respectively, with a grid point spacing of 0.375 Å. Ten different conformations were generated for each ligand scored using Auto Dock Vina functions and were ranked according to their binding energies. Following the docking procedure, in Biovia Discovery Studio Visualizer the binding pockets, H-bonds, and other hydrophobic and electrostatic interactions are shown by using different colours, sticks, ribbons and lines.

**2.4 Result Analysis**

After docking is finished, Vina generates an output and a log file for each of the 4000 ligands. Within the logfiles, there is present binding energies for each of the 10 conformations. Binding affinity is the strength of the non-covalent interaction between two or more molecules, such as a protein receptor and a ligand. This ranges from least to the highest, binding affinity are always in negative and the unit be in kcal/mol. An example of one such generated logfile is shown below.

```
-#############################################################
# If you used AutoDock Vina in your work, please cite:      #
#                                                           #
# O. Trott, A. J. Olson,                                    #
# AutoDock Vina: improving the speed and accuracy of docking #
# with a new scoring function, efficient optimization and   #
# multithreading, Journal of Computational Chemistry 31 (2010) #
# 455-461                                                   #
#                                                           #
# DOI 10.1002/jcc.21334                                     #
#                                                           #
# Please see http://vina.scripps.edu for more information.  #
#############################################################

Output will be 47_ligand_1_out.pdbqt
Detected 8 CPUs
Reading input ... done.
Setting up the scoring function ... done.
Analyzing the binding site ... done.
Using random seed: 594223580
Performing search ... done.
Refining results ... done.

mode |   affinity | dist from best mode
     | (kcal/mol) | rmsd l.b.| rmsd u.b.
-----+------------+----------+----------
   1         -4.8      0.000      0.000
   2         -4.4     19.635     20.312
   3         -4.4     18.238     20.104
   4         -4.1     11.473     12.148
   5         -4.0      2.136      2.987
   6         -3.8     11.862     12.683
   7         -3.8     10.660     11.357
   8         -3.8     19.205     20.543
   9         -3.7     11.571     12.360
  10         -3.7     19.857     20.913
Writing output ... done.
```

***Fig 5**: Docking results of a ligand*

Here the mode stands for the number of conformations of the ligand and each binding affinity with the macromolecule. -4.8kcal/mol is the least binding affinity which correlates to being a stronger, more favorable binding.

Binding energy value for the reference ligand (3J5), which is the endogenous small molecule inhibitor was -8 kcal/mol and the ligands that were selected for the next step of the procedure had to be above -8.0 kJ/mol.

For this step, AI was used to generate code, to find ligands which had a binding score of above -8 kcal/mol and a txt file was created bearing the names of the ligands having that specific requirement. From these 4000 ligands, only 354 ligands had a binding affinity above -8.0 kcal/mol.

Visualization was done for the selected ligands in Biovia Drug Discovery software where 2D diagrams were generated of the interaction between the macromolecule (4W6E) and the ligands. From them, only those ligands were chosen who had matching interaction with the reference molecule (the small molecule inhibitor 3J5) which narrowed down the ligands that we are going to use to 54.

***Table 2**: Interaction type between amino acids and ligand*

| Amino acid (Position of Amino Acid) | Type of Interaction |
|---|---|
| TYR 1226 | Carbon-Hydrogen Bond |
| PRO 1235 | Alkyl |
| PRO 1235 | Pi-Alkyl |
| PRO 1187 | Carbon-Hydrogen Bond |
| PRO 1187 | Pi-Alkyl |

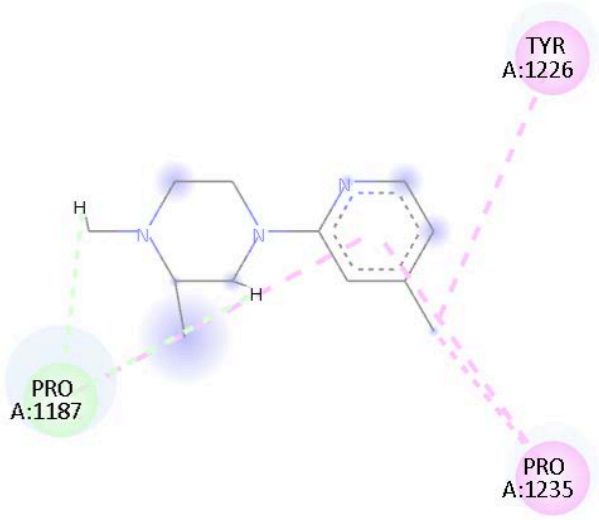


***Fig 6** : 2D diagram for the protein-ligand interaction between 4W6E and 3J5*

| PubChem CID | Compound Name | Binding Energies | Binding Interactions |
|---|---|---|---|
| 3638 | Hydrastinine | -8.0 | Pro1235 Alkyl, Pro1235 Pi-Alkyl, Pro1187 Pi-Alkyl, Pro1187 C–H bond |
| 3797 | ZM-39923 | -8.9 | Pro1235 Pi-Alkyl |
| 4257 | Mosapramine | -8.2 | Pro1235 Alkyl |
| 4578 | 6-(Phenylmethoxy)-9H-purin-2-amine | -8.1 | Pro1235 Pi-Alkyl |
| 5334 | Sulfanitran | -8.4 | Pro1235 Pi-Alkyl, Pro1187 Pi-Alkyl |
| 7019 | 9-Aminoacridine | -8.4 | Pro1187 C–H bond, Pro1235 Pi-Alkyl |
| 9064 | Catechin | -8.7 | Pro1235 Alkyl |
| 9387 | Perfluorooctane | -8.9 | TYR1226 Pi-Alkyl |
| 55223 | Tucaresol | -8.0 | Pro1235 Pi-Alkyl |
| 64949 | Propamidine | -8.2 | Pro1187 Pi-Alkyl |
| 65650 | Litoxetine | -8.8 | Pro1235 Alkyl |
| 70882 | Moxaverine | -8.0 | Pro1235 Pi-Alkyl, TYR1226 Pi-Alkyl |

| | | | |
|---|---|---|---|
| 71132 | Clobenfurol | -8.9 | Pro1235 Pi-Alkyl, Pro1187 Pi-Alkyl |
| 71671 | Benmoxin | -8.2 | Pro1235 Alkyl, TYR1226 Pi-Alkyl, Pro1187 Pi-Alkyl |
| 72099 | Esflurbiprofen | -8.5 | Pro1235 Alkyl, Pro1187 Pi-Alkyl |
| 91766 | Flufenoxuron | -8.2 | TYR1226 Pi-Alkyl, Pro1187 Pi-Alkyl |
| 92093 | Flexzone 6H | -8.3 | Pro1187 Pi-Alkyl |
| 114917 | Tanshinone I | -8.6 | Pro1235 Pi-Alkyl, Pro1187 Pi-Alkyl |
| 148138 | Drug X | -8.3 | Pro1235 Alkyl, TYR1226 Pi-Alkyl |
| 160254 | Cryptotanshinon | -8.1 | Pro1187 Pi-Alkyl |
| 432824 | Oxaflozane | -8.7 | Pro1235 Alkyl |
| 735998 | Clobenzorex | -8.0 | Pro1235 Alkyl, TYR1226 Pi-Alkyl |
| 3086671 | Atreleuton | -8.2 | Pro1235 Alkyl |
| 5282367 | Menatetrenone | -8.3 | Pro1235 Alkyl, TYR1226 Pi-Alkyl |
| 6450806 | Laniquidar | -9.6 | Pro1235 Alkyl, Pro1235 Pi-Alkyl, Pro1187 Pi-Alkyl |
| 9852519 | Avatrombopag | −8.4 | Pro1235 |

| | | | |
|---|---|---|---|
| 9865515 | Mocetinostat | -8.3 | Pro1235 |
| 10220503 | Tasimelteon | -8.0 | TYR1226 Pi-Alkyl |
| 12004316 | PSI-697 | -8.4 | Pro1235 Alkyl, Pro1235 Pi-Alkyl, TYR1226 Pi-Alkyl |
| 16042343 | Crisdesalazine | -8.9 | Pro1235 Alkyl |
| 16719221 | Avutometinib | -8.0 | Pro1235 Pi-Alkyl (×2) |
| 23730143 | MGB-BP-3 | -8.4 | Pro1235 Pi-Alkyl |
| 24737629 | GSK-1521498 | -8.6 | Pro1235 Alkyl, Pro1235 Pi-Alkyl, Pro1187 Pi-Alkyl |
| 24772165 | BNC-210 | -8.6 | Pro1235 Alkyl, Pro1235 Pi-Alkyl, Pro1187 Pi-Alkyl |
| 24812758 | Canagliflozin | -8.6 | Pro1235 Alkyl, Pro1187 C–H bond |
| 24826799 | PONATINIB | -8.4 | Pro1235 Alkyl |
| 24856041 | AMG-900 | -8.2 | Pro1235 Pi-Alkyl |
| 25151352 | Pexidartinib | -9.7 | Pro1235 Alkyl, TYR1226 Pi-Alkyl |
| 46186778 | Snubh-nm-333 F-18 | -8.1 | Pro1235 Pi-Alkyl, Pro1187 Pi-Alkyl |
| 46848036 | Flumatinib | -8.0 | TYR1226 Pi-Alkyl |
| 49836093 | Funapide | -8.9 | Pro1235 Alkyl, Pro1187 Pi-Alkyl |

| | | | |
|---|---|---|---|
| 51049968 | Rimegepant | -8.1 | Pro1235 Pi-Alkyl, Pro1187 Pi-Alkyl |
| 53359074 | BMS-791826 | -8.1 | Pro1235 Alkyl, Pro1235 Pi-Alkyl |
| 56649297 | Fuzuloparib | -8.6 | Pro1235 Pi-Alkyl, TYR1226 Pi-Alkyl |
| 56655833 | TAK-653 | -8.5 | Pro1235 Pi-Alkyl, Pro1187 Pi-Alkyl |
| 56960912 | Cavosonstat | -8.3 | Pro1235 Pi-Alkyl, Pro1187 Pi-Alkyl |
| 58486178 | Ocifisertib | -8.4 | Pro1235 Alkyl, Pro1235 Pi-Alkyl, Pro1187 Pi-Alkyl |
| 70957463 | Flortaucipir F-18 | -8.1 | Pro1235 Pi-Alkyl, Pro1187 Pi-Alkyl |
| 91663352 | Seralutinib | -8.1 | Pro1235 Pi-Alkyl, Pro1187 Pi-Alkyl |
| 118224491 | Emavusertib | -8.0 | Pro1187 Pi-Alkyl |
| 118560618 | Apinocaltamide | -8.4 | Pro1235 Pi-Alkyl, Pro1187 Pi-Alkyl |
| 129103609 | Selitrectinib | -8.0 | Pro1235 Alkyl |
| 135565709 | Adavivint | -9.2 | Pro1187 Pi-Alkyl |
| 139399801 | Vanzacaftor | -8.4 | Pro1235 Alkyl, TYR1226 Pi-Alkyl |

*Table 3: Visualization results and binding interactions between the ligand and receptor molecule*

| PubChem CID | Compound Name | Binding Affinity | Binding Interactions |
|---|---|---|---|
| 135566983 | 3J5 | -8.0 | Pro1235 Alkyl, Pro1235 Pi-Alkyl, Pro1187 Pi-Alkyl, Pro1187 C–H bond |

*Table 4: Visualization results and the binding interactions between 3J5 and receptor molecule*

From the above set of ligands, those demonstrating two or more interaction types in common with the reference ligand protein interaction profile were shortlisted for further consideration. Following this selection process, 31 ligands satisfied the criterion of exhibiting at least two shared interaction types with the target protein. Among these candidates, CID 3638 (Hydrastinine) showed the highest level of similarity to the reference ligand in terms of interaction characteristics and was therefore identified as the most comparable compound within the screened set. Furthermore, we will conduct toxicological analysis for this ligand, alongside the rest of the other ones to predict the physicochemical as well as the pharmacokinetic properties of these ligands.

**2.5 ADME analysis**

During the time- and resource consuming processes of drug discovery and development, a large number of molecular structures are evaluated according to very diverse parameters in order to steer the selection of which chemicals to synthetize, test and promote, with the final goal to identify those with the best chance to become an effective medicine for the patients. The molecules must show high biological activity together with low toxicity. Equally important is the access to and concentration at the therapeutic target in the organism. The traditional way to consider pharmacokinetics to be effective as a drug, a potent molecule must reach its target in the body in sufficient concentration, and stay there in a bioactive form long enough for the expected biologic events to occur. For this reason, drug development involves assessment of absorption,

distribution, metabolism and excretion (ADME) increasingly earlier in the discovery process.(Scotti & Scotti, 2025) It has been demonstrated that early estimation of ADME in the discovery phase reduces drastically the fraction of pharmacokinetics-related failure in the clinical phases. Computer models have been fostered as a valid alternative to experimental procedures for prediction of ADME, especially at initial steps, when investigated chemical structures are numerous but the availability of compounds is scarce.(Ononamadu & Ibrahim, 2021)

In that context, we used the Swiss ADME web tool that gives free access to a pool of fast yet robust predictive models for physicochemical properties, pharmacokinetics, drug-likeness and medicinal chemistry friendliness.

| **Molecule names** | **GI absorption** | **BBB permeant** | **Pgp substrate** | **log Kp (cm/s)** | **Lipinski #violations** |
|---|---|---|---|---|---|
| Vanzacaftor | Low | No | Yes | -6 | 2 |
| Apinocaltamide | High | No | Yes | -6.57 | 0 |
| Seralutinib | High | No | Yes | -6.52 | 0 |
| Flortaucipir F-18 | High | Yes | Yes | -5.56 | 0 |
| CFI-400945 free base | High | No | Yes | -6.2 | 1 |
| Cavosonstat | High | Yes | No | -5.54 | 0 |
| TAK 653 | High | No | No | -6.67 | 0 |
| Fuzuloparib | High | No | Yes | -7.47 | 0 |
| Bms-791826 | Low | No | Yes | -6.27 | 1 |
| Rimegepant | High | No | Yes | -7.93 | 1 |

| | | | | | |
|---|---|---|---|---|---|
| Funapide | High | Yes | Yes | -6.4 | 0 |
| Snubh-nm-333 F-18 | High | Yes | No | -4.79 | 0 |
| Pexidartinib | High | No | Yes | -5.69 | 0 |
| Canagliflozin | High | No | Yes | -6.72 | 0 |
| BNC-210 | High | No | Yes | -6.96 | 0 |
| Gsk-1521498 | High | Yes | Yes | -5.28 | 1 |
| Avutometinib | Low | No | No | -7.44 | 0 |
| Psi-697 | High | Yes | No | -4.37 | 0 |
| Laniquidar | High | No | No | -5.76 | 1 |
| Menatetrenone | High | No | No | -5.76 | 1 |
| Clobenzorex | High | Yes | No | -4.82 | 1 |
| CID 148138 | Low | No | No | -8.81 | 2 |
| Tanshinone I | High | Yes | No | -5.37 | 0 |
| Flufenoxuron | Low | No | Yes | -4.84 | 1 |
| Esflurbiprofen | High | Yes | No | -4.84 | 0 |
| Benmoxin | High | Yes | No | -6.05 | 0 |
| Clobenfurol | High | Yes | Yes | -5.18 | 0 |
| Moxaverine | High | Yes | No | -4.75 | 0 |
| 9-Aminoacridine | High | Yes | Yes | -5.54 | 0 |
| Sulfanitran | High | No | Yes | -6.93 | 0 |
| Hydrastinine | High | No | Yes | -6.82 | 0 |

| Molecule names | CYP1A2 inhibitor | CYP2C19 inhibitor | CYP2C9 inhibitor | CYP2D6 inhibitor | CYP3A4 inhibitor |
|---|---|---|---|---|---|
| Vanzacaftor | No | No | No | No | Yes |
| Apinocaltamide | Yes | Yes | Yes | Yes | Yes |
| Seralutinib | Yes | Yes | Yes | Yes | Yes |
| Flortaucipir F-18 | Yes | No | No | Yes | Yes |
| CFI-400945 free base | No | Yes | Yes | Yes | Yes |
| Cavosonstat | Yes | No | No | No | No |
| TAK 653 | Yes | Yes | Yes | No | No |
| Fuzuloparib | No | Yes | No | No | No |
| Bms-791826 | No | Yes | Yes | No | Yes |
| Rimegepant | No | No | No | Yes | No |
| Funapide | Yes | Yes | Yes | Yes | Yes |
| Snubh-nm-333 F-18 | Yes | Yes | Yes | No | Yes |
| Pexidartinib | Yes | Yes | Yes | Yes | Yes |
| Canagliflozin | Yes | No | No | Yes | No |
| BNC-210 | No | Yes | Yes | Yes | Yes |
| Gsk-1521498 | Yes | Yes | No | Yes | Yes |
| Avutometinib | No | No | No | No | No |
| Psi-697 | Yes | Yes | Yes | No | No |

| | | | | | |
|---|---|---|---|---|---|
| Laniquidar | No | No | No | Yes | No |
| Menatetrenone | No | No | No | Yes | No |
| Clobenzorex | Yes | No | No | Yes | No |
| CID 148138 | No | No | No | No | No |
| Tanshinone I | Yes | Yes | No | No | Yes |
| Flufenoxuron | No | Yes | Yes | No | No |
| Esflurbiprofen | No | No | No | No | No |
| Benmoxin | No | No | No | Yes | No |
| Clobenfurol | Yes | Yes | No | Yes | No |
| Moxaverine | Yes | Yes | Yes | Yes | Yes |
| 9-Aminoacridine | Yes | No | No | No | Yes |
| Sulfanitran | No | No | Yes | No | No |
| Hydrastinine | No | No | No | No | No |

*Table: 5 ADME Results*

**3. Results and Discussion; Relative Comparison of Selected Candidate Ligands for Tankyrase-1 Inhibition**

Structure-based molecular docking with pharmacokinetic profiling was conducted to assess the binding potential and drug-likeness properties of four top candidate ligands (Hydrastinine, PSI-697, Benmoxin, BNC-210) against the catalytic pocket of Tankyrase-1. Given that the binding of ligands to the Tankyrase catalytic domain is a structure-based phenomenon, contacts between these molecules (ligands) and residues Pro1235, Pro1187, and Tyr1226 were given special priority in interactions analysis. Besides docking interaction studies, pharmacokinetic and drug-likeness properties were calculated by Swiss ADME, which includes an assessment of the

compliance with Lipinski's rule of five (rule-of-five), gastrointestinal absorption, lipophilicity (Log P), blood–brain barrier permeability, P-glycoprotein substrate status, cytochrome P450 inhibition profile and BOILED-Egg model prediction. Collectively these descriptors create a unified paradigm for early-stage drug discovery to assess oral bioavailability, tissue distribution behavior, metabolic stability and drug–drug interaction liability

### 3.1 Key parameters involved in Drug Discovery and their physiological importance

Lipinski's rule of five which is one of the most accepted and widely used criteria for assessing oral drug-likeness and membrane permeability. The first rule suggests that compounds with a molecular weight greater than 500 Da, more than 5 hydrogen-bond donors or more than 10 hydrogen-bond acceptors or have a Log P value > 5 would be less likely to exhibit good intestinal absorption or permeation (Lipinski et al., 2001). If a certain compound checks all these boxes only then it will advance into clinical development. Physiologically, these parameters affect passive diffusion through biological membranes including intestinal epithelial cells, hepatocytes, renal tubules and blood–brain barrier. In general, drug molecules that go beyond Lipinski limits have low permeability and poor bioavailability leading to a higher probability of failure in the late stage of drug development. This means that Lipinski compliance is still a primary focus of drug discovery to prioritize compounds for oral bioavailability in the early phase of drug discovery (Lipinski et al., 2001)

Gastrointestinal absorption is another key factor for the effectiveness of an oral drug, which measures the compound's permeability through the intestinal epithelial barrier after oral administration and its entry to systemic circulation. The organs responsible for intestinal absorption guarantee systemically relevant plasma concentrations after oral dosing occurring within therapeutically effective ranges and thus systemic pharmacological activity. Diminished bioavailability, increased dosing requirement and decreased therapeutic effectiveness are common consequences of poor gastrointestinal permeability. So prediction of oral bioavailability using computational means based on some physicochemical properties (polarity, lipophilicity and molecular size) is significant to determine the suitability for gastrointestinal absorption before any experimental determination of pharmacokinetic characteristics.(Koziolek et al., 2019)

Lipophilicity (Generally Log P/ Octanol–water partition Coefficient) is also a critical factor contributing to their absorption and distribution behavior. Log P is a descriptor of the relative lipophilicity of a compound with lipid membranes compared to aqueous biological environments and impacts its membrane permeability, plasma protein binding, metabolic stability and tissue distribution characteristics. Compounds with moderate lipophilicity are usually observed to be ideal for in vivo pharmacokinetic behaviour because this leads to optimal aqueous solubility and yet maximum passive membrane diffusion capacity. Thus, highly lipophilic compounds may demonstrate low solubility and metabolic instability, while excessive lipophobicity may limit barrier penetration and systemic availability. As such, the optimization of Log P remains a central tenet of many medicinal chemistry lead-optimization strategies (Arnott & Planey, 2012; Bruno et al., 2021; Lipinski et al., 2001)

A key pharmacokinetic marker defining the ability of a compound to cross the blood–brain barrier after systemic administration is permeation of the blood–brain barrier. Tightly packed endothelial cells of the blood–brain barrier create a physical and functional fence that inhibits passive transport even of polar/hydrophilic or high-molecular-weight compounds into brain tissue.(Kadry et al., 2020). Such molecules that are permeable across this barrier usually have low polarity with a mid-range molecular weight and an overall intermediate lipophilicity. From a physiological perspective, prediction of blood–brain barrier permeability is critical as compounds targeting central nervous system indications require effective brain penetration while drugs for peripheral targets may actually benefit from low level brain exposure in order to avoid unwanted neurological side-effects. Blood–brain barrier permeability evaluation may give useful direction in determining drug selectivity for particular therapeutic targets, especially early in the development stage

Prediction of P-glycoprotein substrate helps gain an additional insight into the probability of transporter-mediated drug efflux across biological membranes. P-glycoprotein, an ATP-dependent efflux transporter with broad substrate specificity, is expressed in intestine, liver, kidney and blood–brain barrier where it serves major protective functions by limiting intracellular xenobiotic compound accumulation. Drugs that are characterized as P-glycoprotein substrates may be less well absorbed from the intestinal epithelium, have diminished access to the brain, and exhibit decreased intracellular retention, all due to active efflux. As a result,

recognition of P-glycoprotein-substrate profiles during computational pharmacokinetic investigations has recently become important for predicting potential limitations in systemic exposure and tissue distribution (Giacomini et al., 2010).

Cytochrome P450 (CYP) enzymes form the main metabolic pathway of xenobiotic oxidative biotransformation in the liver and inhibition of them is a decisive mechanism implicated in drug–drug interactions and metabolic liability. CYP3A4, CYP2D6, CYP2C9, CYP2C19 and CYP1A2 are the five most clinically relevant isoforms that together metabolize the majority of marketed pharmaceutical compounds. In silico prediction of cytochrome P450 inhibition profiles is an essential metric of metabolic liability, interindividual variability in systemic clearance rates and risk of drug–drug interaction during polytherapy. Lead selection favours compounds that exhibit low inhibition of major cytochrome P450 isoforms, because they will represent a lower risk for challenging pharmacokinetic interactions in the clinical setting (Zanger & Schwab, 2013)

BOILED-Egg model: a graph-based predictive method that is available in SwissADME and predicts passive gastrointestinal permeability and blood–brain barrier penetration from two simple physicochemical descriptors, lipophilicity, s2 28-30 and topological polar surface area (TPSA). Compounds located in the white area of this diagram are expected to possess a low probability of intestinal absorption, and arrows in the yolk area indicate which compounds would presumably cross blood–brain barrier based on the use model. BOILED-Egg model enables fast visualization of pharmacokinetic suitability early in the drug discovery process by determining intestinal permeability, and transporter-mediated efflux behavior to identify (Daina et al., 2017).

### 3.2 Result discussion in accordance to their ADME results

Molecular docking analysis revealed a stable conformational fit of Hydrastinine molecule and the residues Pro1235 and Pro1187 in so far as they formed hydrophobic alkyl or π-alkyl interactions with residue within the catalytic pocket. However, an interaction with Tyr1226 was

not observed indicating less stringent catalytic pocket specificity when compared to ligands binding aromatic residues. While its short half-life is a concern, Hydrastinine also predicted well in terms of pharmacokinetic properties (high gastrointestinal absorption, good aqueous solubility, no cytochrome P450 inhibition and adherence to Lipinski's rule of five). Furthermore, BOILED-Egg analysis predicted Hydrastinine to be within the gastrointestinal absorption zone but outside the blood–brain barrier penetration zone indicating a suitable target for exploratory peripheral therapeutic targeting with diminished central nervous system exposure risk.

Together with predicted π-interaction involving Tyr1226, PSI-697 exhibited hydrophobic interaction with Pro1235, indicating potentially better catalytic pocket specificity over ligands without an aromatic stabilization. Swiss ADME analysis revealed high gastrointestinal absorption and optimal lipophilicity (consensus Log P ≈ 4.31) which favoured possible membrane permeability. BOILED-Egg prediction showed PSI-697 was positioned in both gastrointestinal absorption and blood–brain barrier penetration zones, suggesting a potential for central nervous system (CNS) exposure. Although additional in vitro studies suggest involvement of metabolic interactions that would limit the pharmacokinetic optimization of this compound during further development (e.g., predicted inhibition of multiple cytochrome P450 isoforms such as CYP1A2, CYP2C19 and/or CYP2C9),

Of the ligands assessed, Benmoxin displayed the most extensive predicted catalytic pocket engagement of any compound as it was modeled to simultaneously interact with residues Pro1235, Pro1187 and Tyr1226 demonstrating multi-point anchoring within the binding cavity. Now these interactions patterns are typically related to better stabilization of ligand and higher inhibitory capacity into the active site of enzymes. Swiss ADME profiling was used to confirm good intestinal absorption and acceptable lipophilicity (consensus Log P ≈ 2.60), lack of P-glycoprotein substrate behavior and compliance with Lipinski's rule of five. Both intestinal absorption and blood–brain barrier (BBB) permeability were predicted by BOILED-Egg analysis, supporting its potential pharmacological systemic delivery and access to the central nervous system. The moderate inhibition of CYP2D6 predicted suggests a low risk for metabolic interaction, and the overall pharmacokinetic profile indicates desirable drug-likeness properties suitable for prioritization to further molecular dynamics simulations.

BNC-210 showed hydrophobic interactions with Pro1235 and Pro1187; however, it did not interact with Tyr1226 indicating comparatively less catalytic pocket specificity when compared to Benmoxin and PSI-697. However, Swiss ADME pharmacokinetic profiling predicted high gastrointestinal absorption and ideal lipophilicity (consensus Log P ≈ 2.61), indicating desirable oral drug-like properties. BOILED-Egg analysis predicted potential intestinal absorption and blood–brain barrier penetration, but behavior as a P-glycoprotein substrate may reduce efficiency of intracellular accumulation. Additionally, predicted inhibition of various cytochrome P450 isoforms such as CYP2C19, CYP2C9, CYP2D6 and CYP3A4 indicates likely greater metabolic interaction liability when evaluated against the other candidate ligands examined in this study.

All four ligands complied with Lipinski's rule of five without violation, and their comparative pharmacokinetic evaluation showed high predicted gastrointestinal absorption accordingly these compounds can be considered as suitable orally active small-molecule candidates. Because there is neither inhibition of cytochrome P450 nor any known blood–brain barrier permeability, the predicted metabolic interaction profile for Hydrastinine was deemed to be the safest. Interaction of PSI-697 with Tyr1226 conferred higher catalytic pocket specificity but moderate cytochrome P450 inhibition liability. Benmoxin proved the best combination of an engaged catalytic pocket and well-balanced pharmacokinetic properties for a small-molecule, with desirable lipophilicity and lack of P-glycoprotein substrate activity. While BNC-210 showed favorable translational pharmacokinetic properties, forecasted multi-isoform cytochrome P450 inhibition and susceptibility to P-glycoprotein efflux suggests it is a less suitable clinical candidate as Tankyrase-1 inhibitor than comparators.

In aggregate, the information obtained from performing docking interaction analysis in conjunction with pharmacokinetic and drug-likeness profiling provides evidence that Benmoxin is the most mechanistically viable Tankyrase-1 inhibitor candidate of those ligands assessed with PSI-697 as a specificity-oriented binder via Tyr1226 interaction. Hydrastinine exhibited acceptable metabolic safety features with stable accommodation in the catalytic pocket, while BNC-210 is a second candidate driven primarily by favorable oral pharmacokinetics. This provides rationale for advancing Benmoxin and PSI-697 as top hits to the next stage of molecular dynamics simulation studies examining stability within the Tankyrase-1 catalytic binding domain.

## 4.Future Direction

With the present in silico analysis of Tankyrase I inhibitors for ovarian cancer, we have provided an important computational starting point for selecting candidate ligands, but more experimental approaches must be made to validate and extend these findings. In vitro validation studies with enzyme inhibition assays and ovarian cancer cell line–based studies should also be prioritized in future research as additional evidence of biological activity in the shortlisted compounds confirmed their selectivity. These tests would validate the predicted ligand–protein interactions and determine whether inhibition of Tankyrase I activity occurs along measurable pathways resulting in cancer cell proliferation suppression. Then, preclinical studies in relevant animal models are recommended to test the pharmacokinetic properties, toxicity profiles, and therapeutic efficacy of candidate compounds. This is critical for validating the safety and clinical-transformation of these ligands as drug candidates.

Potential advancements of this research may involve molecular dynamics (MD) simulations enabling the exploration of thermodynamic stability and flexibility as well as ligand–protein complexes over long time spans in a physiological environment. These could also include binding free energy calculations, quantitative structure–activity relationship (QSAR) modeling and even these structure-based drug optimization strategies so as to improve the reliability predictive power of the computational screening results.

Furthermore, answering some questions will help us move forward towards drug development for the candidates mentioned above. For example:

Are the candidate ligands discovered able to inhibit Tankyrase I activity upon Ovarian cancer cell models?

Do these ligands preferentially bind Tankyrase I over the rest of PARP enzyme family members?

What structural modulation could lead to better binding affinity and therapeutic implications?

Is combination therapy with Tankyrase I inhibitors efficacious in ovarian cancer?

This will add translational value to the current results and help move towards drug development.

## 5. Conclusion

This study was aimed at assessing potential Tankyrase I inhibitors from ovarian cancer using methodology which involves computational docking and interaction-based screening. Several candidates chosen from the original set of screened ligands were close matches in binding affinity and interaction to compound C as well AMPK inhibitors with the potential to be useful new therapeutic leads. More precisely, discovered ligands with many common modes of interactions with the reference compound means high similarity to docking poses in the active site of target protein.

This work shows that phase in silico studies are an effective guide to expedite drug discovery anticancer screening compared to classical approaches, which are time consuming and costly. Through this research, it may conserve time and effort by cutting down a large pool of compounds into a handful of promising candidates that could give physiological validation and help to optimize biological stability.

Most importantly, this study not only supports the further evaluation of Tankyrase I as a therapeutic target in ovarian cancer but also exemplifies use of systematic computational screening strategies to validate druggable phenotypes and make progress towards the targeted discovery of drugs. This information could help researchers to design the next generation of more specific drugs and provide new options for patients suffering from ovarian cancer.All in all, the study provides a foundation for identifying potential Tankyrase I inhibitors using computational methods and acts as a spring board for experimental validation and drug development.

## References


Arend, R. C., Londoño-Joshi, A. I., Straughn, J. M., Jr., & Buchsbaum, D. J. (2013). The Wnt/β-catenin pathway in ovarian cancer: A review. *Gynecologic Oncology*, *131*(3), 772–779. https://doi.org/10.1016/j.ygyno.2013.09.034

Arend, R. C., Londoño-Joshi, A. I., Straughn, J. M., Jr., & Buchsbaum, D. J. (2013). The Wnt/β-catenin pathway in ovarian cancer: a review. *Gynecol Oncol*, *131*(3), 772–779. https://doi.org/10.1016/j.ygyno.2013.09.034

Arnott, J. A., & Planey, S. L. (2012). The influence of lipophilicity in drug discovery and design. *Expert Opin Drug Discov*, *7*(10), 863–875. https://doi.org/10.1517/17460441.2012.714363

Braicu, E. I., Sehouli, J., Richter, R., Pietzner, K., Denkert, C., & Fotopoulou, C. (2011). Role of histological type on surgical outcome and survival following radical primary tumour debulking of epithelial ovarian, fallopian tube and peritoneal cancers. *Br J Cancer*, *105*(12), 1818–1824. https://doi.org/10.1038/bjc.2011.455

Bruno, C. D., Harmatz, J. S., Duan, S. X., Zhang, Q., Chow, C. R., & Greenblatt, D. J. (2021). Effect of lipophilicity on drug distribution and elimination: Influence of obesity. *Br J Clin Pharmacol*, *87*(8), 3197–3205. https://doi.org/10.1111/bcp.14735

Caruso, G., Weroha, S. J., & Cliby, W. (2025). Ovarian Cancer: A Review. *JAMA*, *334*(14), 1278–1291. https://doi.org/10.1001/jama.2025.9495

Cho, K. R., & Shih, I.-M. (2009). Ovarian Cancer. *Annual Review of Pathology: Mechanisms of Disease*, *4*(Volume 4, 2009), 287–313. https://doi.org/https://doi.org/10.1146/annurev.pathol.4.110807.092246

Chornokur, G., Amankwah, E. K., Schildkraut, J. M., & Phelan, C. M. (2013). Global ovarian cancer health disparities. *Gynecol Oncol*, *129*(1), 258–264. https://doi.org/10.1016/j.ygyno.2012.12.016

Çifci, G., Aviyente, V., & Akten, E. D. (2012). Molecular Docking Study Based on Pharmacophore Modeling for Novel PhosphodiesteraseIV Inhibitors. *Molecular Informatics*, *31*(6-7), 459–471. https://doi.org/https://doi.org/10.1002/minf.201100141

Filho, A. M., Laversanne, M., Ferlay, J., Colombet, M., Piñeros, M., Znaor, A., Parkin, D. M., Soerjomataram, I., & Bray, F. (2025). The GLOBOCAN 2022 cancer estimates: Data sources, methods, and a snapshot of the cancer burden worldwide. *International Journal of Cancer*, *156*(7), 1336–1346. https://doi.org/https://doi.org/10.1002/ijc.35278

Haikarainen, T., Krauss, S., & Lehtio, L. (2014). Tankyrases: structure, function and therapeutic implications in cancer. *Curr Pharm Des*, *20*(41), 6472–6488. https://doi.org/10.2174/1381612820666140630101525

Haikarainen, T., Waaler, J., Ignatev, A., Nkizinkiko, Y., Venkannagari, H., Obaji, E., Krauss, S., & Lehtiö, L. (2016). Development and structural analysis of adenosine site binding tankyrase inhibitors. *Bioorganic & Medicinal Chemistry Letters*, *26*(2), 328–333. https://doi.org/https://doi.org/10.1016/j.bmcl.2015.12.018

Harris, P. J., Speranza, G., & Dansky Ullmann, C. (2012). Targeting embryonic signaling pathways in cancer therapy. *Expert Opin Ther Targets*, *16*(1), 131–145. https://doi.org/10.1517/14728222.2011.645808

Jones, S., Wang, T. L., Shih Ie, M., Mao, T. L., Nakayama, K., Roden, R., Glas, R., Slamon, D., Diaz, L. A., Jr., Vogelstein, B., Kinzler, K. W., Velculescu, V. E., & Papadopoulos, N. (2010). Frequent mutations of chromatin remodeling gene ARID1A in ovarian clear cell carcinoma. *Science*, *330*(6001), 228–231. https://doi.org/10.1126/science.1196333

Kadry, H., Noorani, B., & Cucullo, L. (2020). A blood-brain barrier overview on structure, function, impairment, and biomarkers of integrity. *Fluids Barriers CNS*, *17*(1), 69. https://doi.org/10.1186/s12987-020-00230-3

Kikuchi, A. (2003). Tumor formation by genetic mutations in the components of the Wnt signaling pathway. *Cancer Sci*, *94*(3), 225–229. https://doi.org/10.1111/j.1349-7006.2003.tb01424.x

Kikuchi, A., Yamamoto, H., & Kishida, S. (2007). Multiplicity of the interactions of Wnt proteins and their receptors. *Cellular Signalling*, *19*(4), 659–671. https://doi.org/https://doi.org/10.1016/j.cellsig.2006.11.001

Knudsen, S., Nielsen, A., Jensen, T., Gimsing, P., Hansen, A., Madsen, M. W., Gargano, M., Iglesias, J., Musa, F., Moore, K. N., & Graff, J. (2026). Abstract 2454: A Drug Response Predictor (DRP®) is associated with enhanced overall survival in the phase 2 trial in advanced, recurrent ovarian cancer patients treated twice daily with 2X-121/ Stenoparib (NCT03878849). *Cancer Research*, *86*(7_Supplement), 2454–2454. https://doi.org/10.1158/1538-7445.Am2026-2454

Kobayashi, H., Kajiwara, H., Kanayama, S., Yamada, Y., Furukawa, N., Noguchi, T., Haruta, S., Yoshida, S., Sakata, M., Sado, T., & Oi, H. (2009). Molecular pathogenesis of endometriosis-associated clear cell carcinoma of the ovary (review). *Oncol Rep*, *22*(2), 233–240.

Koshiyama, M., Matsumura, N., & Konishi, I. (2017). Subtypes of Ovarian Cancer and Ovarian Cancer Screening. *Diagnostics (Basel)*, *7*(1). https://doi.org/10.3390/diagnostics7010012

Kossaï, M., Leary, A., Scoazec, J. Y., & Genestie, C. (2018). Ovarian Cancer: A Heterogeneous Disease. *Pathobiology*, *85*(1-2), 41–49. https://doi.org/10.1159/000479006

Koziolek, M., Alcaro, S., Augustijns, P., Basit, A. W., Grimm, M., Hens, B., Hoad, C. L., Jedamzik, P., Madla, C. M., Maliepaard, M., Marciani, L., Maruca, A., Parrott, N., Pávek, P., Porter, C. J. H., Reppas, C., van Riet-Nales, D., Rubbens, J., Statelova, M.,…Corsetti, M. (2019). The mechanisms of pharmacokinetic food-drug interactions - A perspective from the UNGAP group. *Eur J Pharm Sci*, *134*, 31–59. https://doi.org/10.1016/j.ejps.2019.04.003

Kuntz, I. D., Blaney, J. M., Oatley, S. J., Langridge, R., & Ferrin, T. E. (1982). A geometric approach to macromolecule-ligand interactions. *J Mol Biol*, *161*(2), 269–288. https://doi.org/10.1016/0022-2836(82)90153-x

Kuo, K. T., Mao, T. L., Jones, S., Veras, E., Ayhan, A., Wang, T. L., Glas, R., Slamon, D., Velculescu, V. E., Kuman, R. J., & Shih Ie, M. (2009). Frequent activating mutations of PIK3CA in ovarian clear cell carcinoma. *Am J Pathol*, *174*(5), 1597–1601. https://doi.org/10.2353/ajpath.2009.081000

La Vecchia, C. (2001). Epidemiology of ovarian cancer: a summary review. *Eur J Cancer Prev*, *10*(2), 125–129. https://doi.org/10.1097/00008469-200104000-00002

Lee, Y. Y., Kim, T. J., Kim, M. J., Kim, H. J., Song, T., Kim, M. K., Choi, C. H., Lee, J. W., Bae, D. S., & Kim, B. G. (2011). Prognosis of ovarian clear cell carcinoma compared to other histological subtypes: a meta-analysis. *Gynecol Oncol*, *122*(3), 541–547. https://doi.org/10.1016/j.ygyno.2011.05.009

Lipinski, C. A., Lombardo, F., Dominy, B. W., & Feeney, P. J. (2001). Experimental and computational approaches to estimate solubility and permeability in drug discovery and development settings. *Adv Drug Deliv Rev*, *46*(1-3), 3–26. https://doi.org/10.1016/s0169-409x(00)00129-0

Lu, F. I., Gilks, C. B., Mulligan, A. M., Ryan, P., Allo, G., Sy, K., Shaw, P. A., Pollett, A., & Clarke, B. A. (2012). Prevalence of loss of expression of DNA mismatch repair proteins in primary epithelial ovarian tumors. *Int J Gynecol Pathol*, *31*(6), 524–531. https://doi.org/10.1097/PGP.0b013e31824fe2aa

Lu, P.-S., Pan, Z.-N., Pan, W.-L., Zou, Y.-J., Ma, R.-J., Zhang, K.-H., Wang, Y., & Sun, S.-C. (2026). Tankyrase activity is essential for asymmetric division and chromosome segregation in oocyte meiosis. *Journal of Advanced Research*, *82*, 315–330. https://doi.org/https://doi.org/10.1016/j.jare.2025.07.008

Ludwick, C., Gilks, C. B., Miller, D., Yaziji, H., & Clement, P. B. (2005). Aggressive behavior of stage I ovarian mucinous tumors lacking extensive infiltrative invasion: a report of four cases and review of the literature. *Int J Gynecol Pathol*, *24*(3), 205–217. https://doi.org/10.1097/01.pgp.0000159935.38913.57

Malpica, A., Deavers, M. T., Lu, K., Bodurka, D. C., Atkinson, E. N., Gershenson, D. M., & Silva, E. G. (2004). Grading ovarian serous carcinoma using a two-tier system. *Am J Surg Pathol*, *28*(4), 496–504. https://doi.org/10.1097/00000478-200404000-00009

Martins-Neves, S. R., Paiva-Oliveira, D. I., Fontes-Ribeiro, C., Bovée, J., Cleton-Jansen, A. M., & Gomes, C. M. F. (2018). IWR-1, a tankyrase inhibitor, attenuates Wnt/β-catenin signaling in cancer stem-like cells and inhibits in vivo the growth of a subcutaneous human osteosarcoma xenograft. *Cancer Lett*, *414*, 1–15. https://doi.org/10.1016/j.canlet.2017.11.004

Mayr, D., Hirschmann, A., Löhrs, U., & Diebold, J. (2006). KRAS and BRAF mutations in ovarian tumors: a comprehensive study of invasive carcinomas, borderline tumors and extraovarian implants. *Gynecol Oncol*, *103*(3), 883–887. https://doi.org/10.1016/j.ygyno.2006.05.029

Mitra, T., & Roy, S. S. (2017). Co-Activation of TGFβ and Wnt Signalling Pathways Abrogates EMT in Ovarian Cancer Cells. *Cell Physiol Biochem*, *41*(4), 1336–1345. https://doi.org/10.1159/000464436

Momenimovahed, Z., Tiznobaik, A., Taheri, S., & Salehiniya, H. (2019). Ovarian cancer in the world: epidemiology and risk factors. *Int J Womens Health*, *11*, 287–299. https://doi.org/10.2147/ijwh.S197604

Moore, K. N., Angelergues, A., Konecny, G. E., García, Y., Banerjee, S., Lorusso, D., Lee, J.-Y., Moroney, J. W., Colombo, N., Roszak, A., Tromp, J., Myers, T., Lee, J.-W., Beiner, M., Cosgrove, C. M., Cibula, D., Martin, L. P., Sabatier, R., Buscema, J.,…Gorp, T. V. (2023). Mirvetuximab Soravtansine in FRα-Positive, Platinum-Resistant Ovarian Cancer. *New England Journal of Medicine*, *389*(23), 2162–2174. https://doi.org/doi:10.1056/NEJMoa2309169

Narwal, M., Fallarero, A., Vuorela, P., & Lehtiö, L. (2012). Homogeneous Screening Assay for Human Tankyrase. *SLAS Discovery*, *17*(5), 593–604. https://doi.org/10.1177/1087057112436558

O'Boyle, N. M., Banck, M., James, C. A., Morley, C., Vandermeersch, T., & Hutchison, G. R. (2011). Open Babel: An open chemical toolbox. *J Cheminform*, *3*, 33. https://doi.org/10.1186/1758-2946-3-33

Ononamadu, C. J., & Ibrahim, A. (2021). Molecular docking and prediction of ADME/drug-likeness properties of potentially active antidiabetic compounds isolated from aqueous-methanol extracts of Gymnema sylvestre and Combretum micranthum. *BioTechnologia (Pozn)*, *102*(1), 85–99. https://doi.org/10.5114/bta.2021.103765

Prasada Rao, C. M., Silakabattini, K., Narapusetty, N., Marabathuni, V. J. P., Thejomoorthy, K., Rajeswari, T., & Y, S. (2023). Insights from the molecular docking and simulation analysis of P38 MAPK phytochemical inhibitor complexes. *Bioinformation*, *19*(3), 323–330. https://doi.org/10.6026/97320630019323

Rodríguez, I. M., & Prat, J. (2002). Mucinous tumors of the ovary: a clinicopathologic analysis of 75 borderline tumors (of intestinal type) and carcinomas. *Am J Surg Pathol*, *26*(2), 139–152. https://doi.org/10.1097/00000478-200202000-00001

Scotti, L., & Scotti, M. T. (2025). ADME Properties in Drug Delivery. *Pharmaceutics*, *17*(5). https://doi.org/10.3390/pharmaceutics17050617

Seeliger, D., & de Groot, B. L. (2010). Ligand docking and binding site analysis with PyMOL and Autodock/Vina. *J Comput Aided Mol Des*, *24*(5), 417–422. https://doi.org/10.1007/s10822-010-9352-6

Trott, O., & Olson, A. J. (2010). AutoDock Vina: improving the speed and accuracy of docking with a new scoring function, efficient optimization, and multithreading. *J Comput Chem*, *31*(2), 455–461. https://doi.org/10.1002/jcc.21334

Trott, O., & Olson, A. J. (2010). AutoDock Vina: Improving the speed and accuracy of docking with a new scoring function, efficient optimization, and multithreading. *Journal of Computational Chemistry*, *31*(2), 455–461. https://doi.org/https://doi.org/10.1002/jcc.21334

van Zundert, G. C. P., Rodrigues, J., Trellet, M., Schmitz, C., Kastritis, P. L., Karaca, E., Melquiond, A. S. J., van Dijk, M., de Vries, S. J., & Bonvin, A. (2016). The HADDOCK2.2 Web Server: User-Friendly Integrative Modeling of Biomolecular Complexes. *J Mol Biol*, *428*(4), 720–725. https://doi.org/10.1016/j.jmb.2015.09.014

Vang, R., Shih Ie, M., & Kurman, R. J. (2009). Ovarian low-grade and high-grade serous carcinoma: pathogenesis, clinicopathologic and molecular biologic features, and diagnostic problems. *Adv Anat Pathol*, *16*(5), 267–282. https://doi.org/10.1097/PAP.0b013e3181b4fffa

Wang, Q., Li, L., You, L., Wang, S., Han, L., Wang, B., Yao, L., Lu, Y., Mender, I., Flusche, A. M., Kim, C., Yarravarapu, N., Lemoff, A., Lum, L., Shay, J. W., Yu, Y., & Chen, C. (2025). Role of tankyrase scaffolding in the β-catenin destruction complex and WNT signaling. *bioRxiv*, 2025.2009.2022.677768. https://doi.org/10.1101/2025.09.22.677768

Wu, X., Luo, F., Li, J., Zhong, X., & Liu, K. (2016). Tankyrase 1 inhibitior XAV939 increases chemosensitivity in colon cancer cell lines via inhibition of the Wnt signaling pathway. *Int J Oncol*, *48*(4), 1333–1340. https://doi.org/10.3892/ijo.2016.3360

Yamashita, Y., Nagasaka, T., Naiki-Ito, A., Sato, S., Suzuki, S., Toyokuni, S., Ito, M., & Takahashi, S. (2015). Napsin A is a specific marker for ovarian clear cell adenocarcinoma. *Mod Pathol*, *28*(1), 111–117. https://doi.org/10.1038/modpathol.2014.61

Zanger, U. M., & Schwab, M. (2013). Cytochrome P450 enzymes in drug metabolism: regulation of gene expression, enzyme activities, and impact of genetic variation. *Pharmacol Ther*, *138*(1), 103–141. https://doi.org/10.1016/j.pharmthera.2012.12.007

Zhu, H., Gao, Y., Liu, L., Tao, M., Lin, X., Cheng, Y., Shen, Y., Xue, H., Guan, L., Zhao, H., Liu, L., Wang, S., Yang, F., Zhou, Y., Liao, H., Sun, F., & Lin, H. (2024). A novel TNKS/USP25 inhibitor blocks the Wnt pathway to overcome multi-drug resistance in TNKS-overexpressing colorectal cancer. *Acta Pharm Sin B*, *14*(1), 207–222. https://doi.org/10.1016/j.apsb.2023.10.013